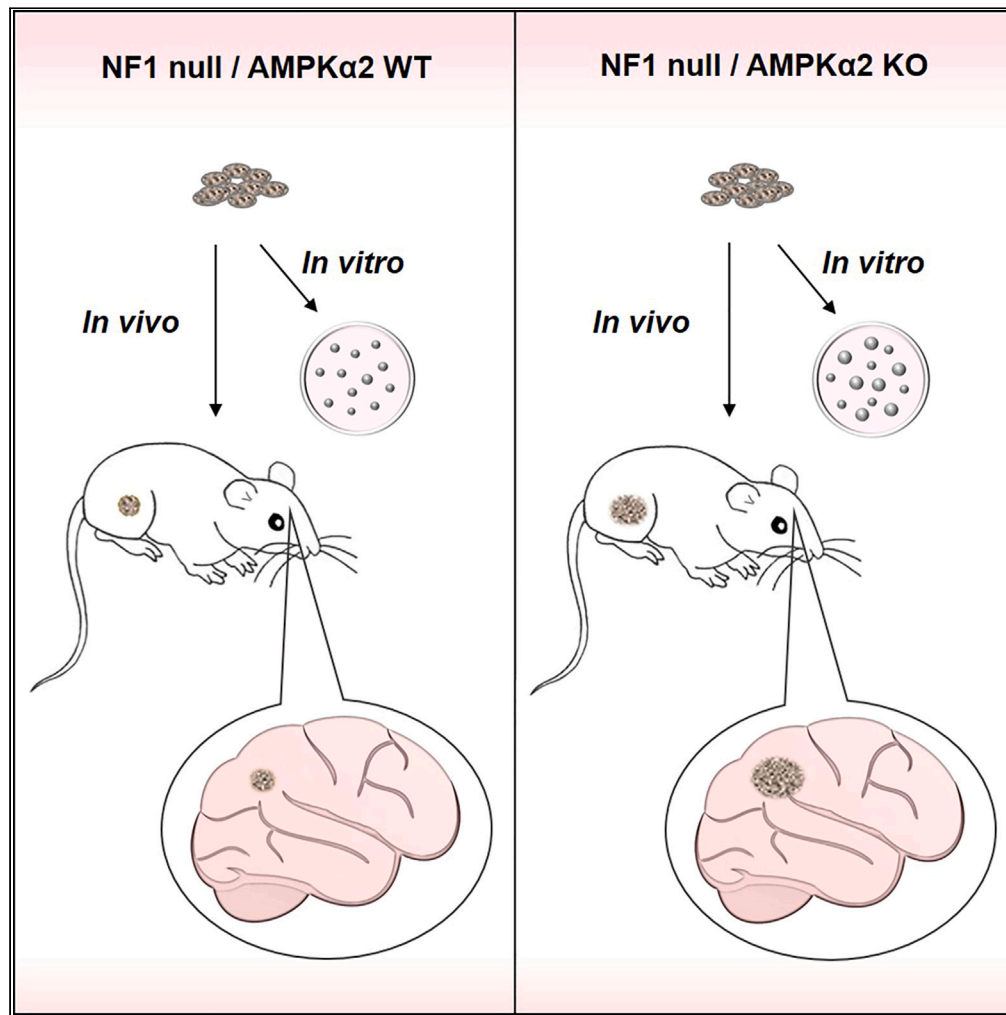


Article

Loss of AMPK α 2 promotes melanoma tumor growth and brain metastasis



Ping Yuan, Da Teng, Evelyn de Groot, ..., Michael A. Davies, Y.N. Vashisht Gopal, Bin Zheng

bin.zheng@cbr2.mgh.harvard.edu

Highlights

AMPK α 2 mutations frequently occur in melanomas, often together with *NF1* mutations

Loss of AMPK α 2 accelerated tumor growth of *NF1*-mutant melanoma in nude mice

AMPK α 2 levels are lower in melanoma brain metastasis than extracranial metastases

Loss of AMPK α 2 enhanced brain metastasis of *NF1*-mutant melanoma in mice

Yuan et al., iScience 26, 106791
June 16, 2023 © 2023 The Author(s).
<https://doi.org/10.1016/j.isci.2023.106791>



Article

Loss of AMPK α 2 promotes melanoma tumor growth and brain metastasis

Ping Yuan,^{1,3} Da Teng,¹ Evelyn de Groot,² Man Li,¹ Sebastian Trousil,¹ Che-Hung Shen,¹ Jason Roszik,² Michael A. Davies,² Y.N. Vashisht Gopal,² and Bin Zheng^{1,4,*}

SUMMARY

AMP-activated protein kinase (AMPK) is a critical cellular energy sensor at the interface of metabolism and cancer. However, the role of AMPK in carcinogenesis remains unclear. Here, through analysis of the TCGA melanoma dataset, we found that *PRKAA2* gene that encodes the α 2 subunit of AMPK is mutated in ~9% of cutaneous melanomas, and these mutations tend to co-occur with *NF1* mutations. Knockout of AMPK α 2 promoted anchorage-independent growth of *NF1*-mutant melanoma cells, whereas ectopic expression of AMPK α 2 inhibited their growth in soft agar assays. Moreover, loss of AMPK α 2 accelerated tumor growth of *NF1*-mutant melanoma and enhanced their brain metastasis in immune-deficient mice. Our findings support that AMPK α 2 serves as a tumor suppressor in *NF1*-mutant melanoma and suggest that AMPK could be a therapeutic target for treating melanoma brain metastasis.

INTRODUCTION

Melanoma is an aggressively metastasizing disease that arises from melanocytes.¹ There are four major genetic subtypes of cutaneous melanoma: *BRAF*-mutant (41.6%), *NRAS*-mutant (27.7%), *NF1*-mutant (23.1%), and triple wild type.² Compared to *BRAF*- or *NRAS*-mutant melanomas, *NF1*-mutant melanoma is much less studied. The *NF1* tumor suppressor encodes neurofibromin protein that serves as a GTPase-activating protein for RAS. Loss or mutation of *NF1* tumor suppressor results in hyperactivation of the RAS-RAF-MEK-ERK signaling cascade. However, *NF1* mutation alone is not sufficient to initiate malignant transformation of melanocyte.^{3,4} While *BRAF* inhibitors and MEK inhibitors show significant clinical efficacy against *BRAF*-mutant melanomas, there are currently no approved targeted treatments for patients with *NF1*-mutant melanoma. Improved understanding of the biology of *NF1*-mutant melanoma will facilitate development of effective therapeutic strategies for affected patients.

AMP-activated protein kinase (AMPK) plays a central role in maintaining energy homeostasis as a sensor of cellular energy levels in both normal and transformed cells.⁵ AMPK is a heterotrimer consisting of α , β , and γ subunits. The catalytic α subunit has two isoforms in mammals, α 1 and α 2, which are encoded by *PRKAA1* and *PRKAA2*, respectively. The different isoforms of the regulatory subunits β (β 1/ β 2) and γ (γ 1/ γ 2/ γ 3) are encoded by *PRKAB1* and *PRKAB2*, and by *PRKAG1*, *PRKAG2*, and *PRKAG3*, respectively. AMPK is activated under various energy stress conditions, such as glucose deprivation, hypoxia, and other perturbations in energy metabolism. Full activation of AMPK requires binding of AMP/ADP to the γ subunit and phosphorylation of the α subunit by upstream activating kinases, including the tumor suppressor LKB1 (liver kinase B1). Mounting evidence supports that the LKB1-AMPK pathway is one of the major players at the interface of metabolism and cancer.⁶⁻⁹ This notion is not only based on the fact that AMPK is well positioned to monitor metabolic changes in cancer cells but also on the observation that AMPK negatively regulates growth, proliferation, and survival of cancer cells. However, some recent studies suggest that AMPK may also promote tumor growth in certain contexts.¹⁰⁻¹⁴ It remains to be seen whether these effects of AMPK loss are dependent on certain cellular/genetic contexts, tumor types, or particular AMPK complex $\alpha\beta\gamma$ subunit composition. Evidence from human cancer genetics would clarify the roles of AMPK in tumor development and progression.

Here, we report that *PRKAA2* (encoding AMPK α 2) is frequently mutated and lost in *NF1*-mutant melanomas. Loss of AMPK α 2 promotes anchorage-independent growth of *NF1*-mutant melanoma cells *in vitro*, tumor growth and brain metastasis *in vivo* in immune-deficient mice. These data support that AMPK α 2 serves as a tumor suppressor in *NF1*-mutant melanoma.

¹Cutaneous Biology Research Center, Massachusetts General Hospital and Harvard Medical School, Charlestown, MA, USA

²Department of Melanoma Medical Oncology, University of Texas MD Anderson Cancer Center, Houston, TX, USA

³Present address: Department of Biochemistry and Molecular Biology, Tongji Medical College, Huazhong University of Science and Technology, Wuhan, 430030, China

⁴Lead contact

*Correspondence: bin.zheng@cbr2.mgh.harvard.edu

<https://doi.org/10.1016/j.isci.2023.106791>



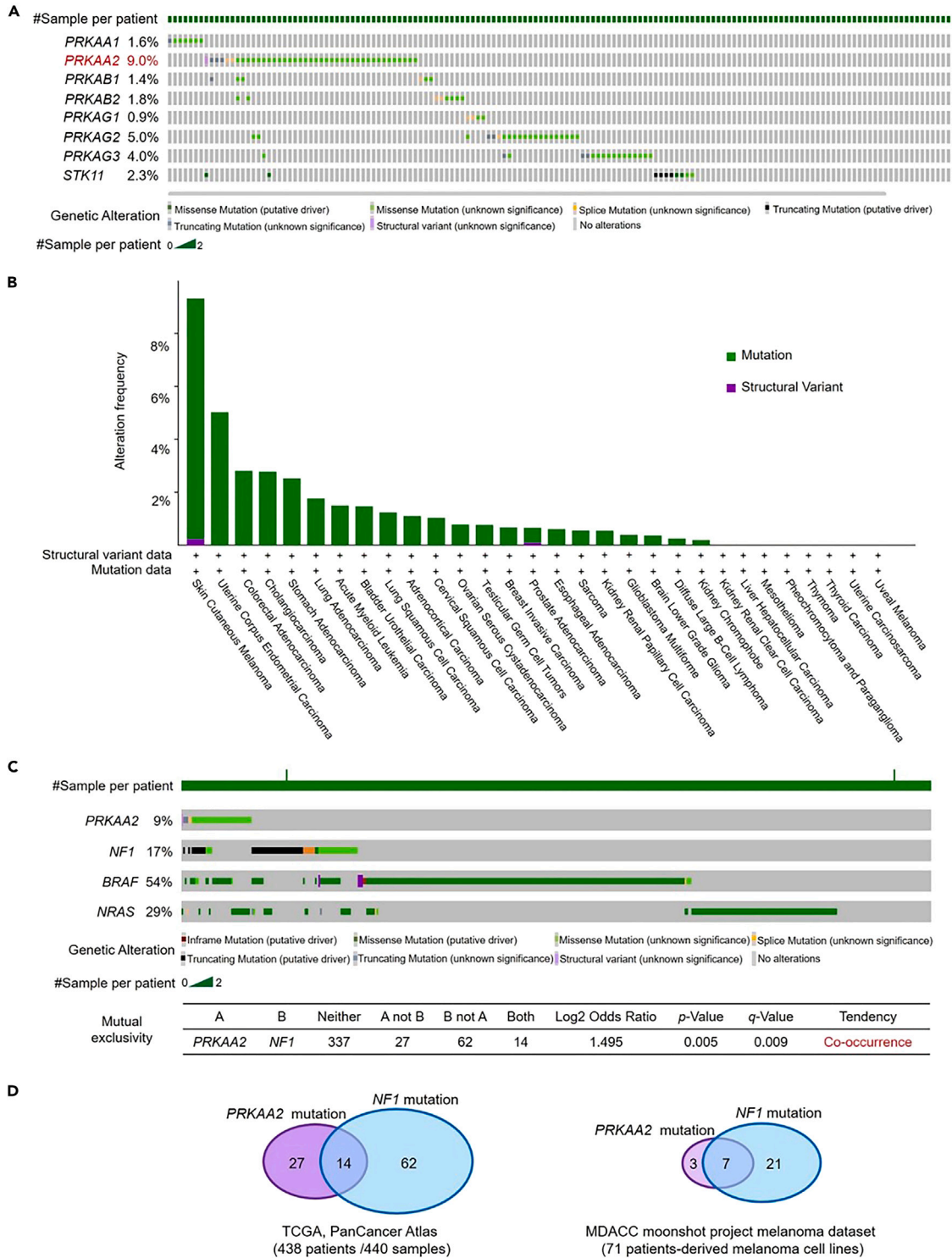


Figure 1. Mutations of PRKAA2 co-occur with NF1 mutations in melanoma

(A) Mutations in various AMPK subunits observed in the Skin Cutaneous Melanoma dataset (TCGA PanCancer Atlas). 438 patients/440 samples with mutation data were analyzed by cBioPortal (www.cbioportal.org). Each column represents a single sample. Different mutation types are shown in different colors as indicated.

(B) Alteration frequency of mutation and structural variant in PRKAA2 gene in multiple cancer types (TCGA, PanCancer Atlas). 30 cancer datasets were analyzed by cBioPortal.

Figure 1. Continued

(C) Mutation or structural variant in *PRKAA2* and *BRAF*, *NRAS*, and *NF1* genes observed in the Skin Cutaneous Melanoma TCGA dataset (TCGA PanCancer Atlas). The co-occurrence of every 2 genes of above 4 genes was analyzed by cBioPortal, and only the co-occurrence of *NF1* and *PRKAA2* mutation is significant (p Value, 0.005).

(D) Co-occurrence of *PRKAA2* mutation and *NF1* mutation in melanoma samples. Melanoma samples from TCGA PanCancer Atlas, or patient-derived melanoma cell lines from MDACC moonshot project dataset contains both *NF1* or/and *PRKAA2* mutations were taken into analysis. Left panel: TCGA PanCancer Atlas; Right panel: MDACC moonshot project dataset.

RESULTS***PRKAA2* is frequently mutated in melanoma**

To explore the role of AMPK in melanoma, we analyzed the mutation status of genes encoding various AMPK subunits in the cutaneous melanoma TCGA dataset (TCGA PanCancer Atlas, 438 patients/440 samples with mutation data) by using cBioPortal.^{15,16} Interestingly, we found that *PRKAA2*, which encodes the $\alpha 2$ isoform of the catalytic subunit of AMPK, is mutated in about 9% of cutaneous melanomas (Figure 1A). Mutation in the $\alpha 1$ isoform of catalytic subunit, *PRKAA1*, was detected in only 1.6%. Mutations in genes encoding two of the regulatory subunits, *PRKAG2* and *PRKAG3*, were detected in 5% and 4%, respectively, of melanomas and in a non-overlapping pattern. Mutations in the other regulatory subunit genes, or the gene encoding *STK11/LKB1*, the major upstream kinase of AMPK, are much rarer (Figure 1A). Analysis of the TCGA PanCancer Atlas showed that melanoma had the highest rate of *PRKAA2* mutations among all cancers in the cohort, with most having mutation rates $\leq 1\%$ (Figure 1B).

Mutations of *PRKAA2* co-occur with *NF1* mutations in melanoma

Next, we examined the mutation pattern of *PRKAA2* in the skin cutaneous melanoma dataset (TCGA, PanCancer Atlas) and their relationship to mutations in the key drivers *BRAF*, *NRAS*, and *NF1*. Strikingly, *PRKAA2* mutations co-occurred with *NF1* mutations (p value, 0.005) (Figure 1C). Among the 41 samples with *PRKAA2* mutation, 14 (34%) also harbored an *NF1* mutation (Figure 1D). In addition to the TCGA dataset, we also analyzed two previously published cohorts of melanoma metastases and patient-derived cell lines with available whole-exome sequencing data.^{17,18} *PRKAA2* mutations were detected in 10 (14%) of 71 patient-derived melanoma cell lines; 7 of them had a concurrent *NF1* mutation (Figure 1D). Furthermore, we examined the levels of AMPK proteins in several established *NF1*-mutant human melanoma cell lines. Loss of AMPK $\alpha 2$ protein, but not $\alpha 1$, was detected in 3 out of 7 lines, including SK-Mel-113, SK-Mel-217, and SK-Mel-103 cells (Figure 2A).

Most *PRKAA2* alterations in the melanoma TCGA dataset are truncating or missense mutations. The mutation sites spread over the entire coding region with no particular hot spot loci, which is consistent with the possibility of loss-of-function (LOF) impact of the mutations. To further determine whether these *PRKAA2* mutations impact AMPK function, we established stable cell lines of AMPK-null DKO (AMPK $\alpha 1/\alpha 2$ double knockout) mouse embryonic fibroblasts (MEFs) expressing wild-type (WT) AMPK $\alpha 2$ or selected cancer-associated mutations (missense E168K and nonsense K379*). As shown in Figure 2B, cells expressing either E168K or K379* mutant AMPK $\alpha 2$ had markedly lower levels of phospho-acetyl-CoA carboxylase, a well-established substrate of AMPK, compared to WT AMPK $\alpha 2$ in response to treatment of AICAR, an AMP mimetic and activator of AMPK. These findings together support that AMPK $\alpha 2$ loss occurs frequently in cutaneous melanoma, particularly in the *NF1*-mutant subtype.

Loss of AMPK $\alpha 2$ promotes *NF1*-mutant melanoma cell anchorage-independent growth *in vitro* and tumor growth in nude mice

To further examine the role of AMPK $\alpha 2$ in melanomagenesis, we knocked out the expression of AMPK $\alpha 2$ in *NF1*-mutant Mewo and WM3918 melanoma cells via the CRISPR-Cas9 approach. We did not observe impact of AMPK $\alpha 2$ knockout (KO) on anchorage-dependent proliferation in 2D culture conditions (Figure S1). However, knockout of AMPK $\alpha 2$ significantly increased anchorage-independent growth of Mewo and WM3918 melanoma cells (Figures 3A and 3D). In addition, we constructed *NF1* KO or/and AMPK $\alpha 1/2$ KO via the CRISPR-Cas9 approach in immortalized human melanocytes. Knockout of AMPK $\alpha 2$, but not AMPK $\alpha 1$, greatly promoted anchorage-independent growth of control melanocytes and *NF1* KO melanocytes (Figures 3E, 3F, and S2). To further confirm the role of AMPK $\alpha 2$ in anchorage-independent growth of melanoma, we ectopically expressed FLAG-AMPK $\alpha 2$ in SK-Mel-113 melanoma cells that are deficient in both *NF1* and AMPK $\alpha 2$ (Figure 2A). Expression of AMPK $\alpha 2$ significantly reduced soft agar colony formation, consistent with inhibition of anchorage-independent growth (Figures 3G and 3H).

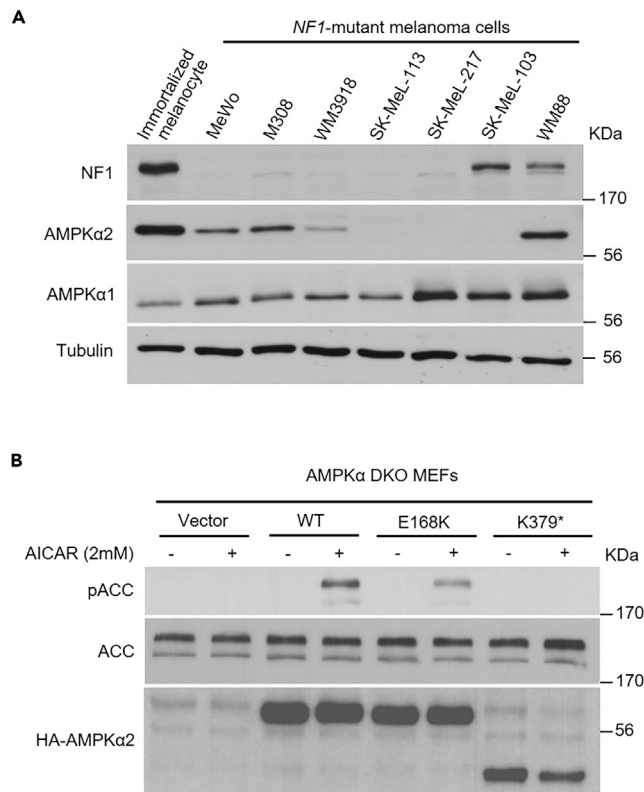


Figure 2. Loss of AMPKα2 in NF1-mutant melanoma cells

(A) Expression of AMPKα2 and AMPKα1 proteins in various NF1-mutant melanoma cells. Various melanoma cells or immortalized human melanocytes were lysed for immunoblotting analysis with indicated antibodies. (B) Immortalized mouse embryonic fibroblasts (AMPKα1/2 DKO MEFs) stably expressing vector (pLHCX), HA-tagged AMPKα2 WT or mutants (E168K, K379*) were treated with 2 mM AICAR for 2 h, followed up with immunoblotting analyses of cell lysates using indicated antibodies.

Based on these results, we evaluated the impact of AMPKα2 on melanoma tumor growth *in vivo*. Scramble or AMPKα2 KO of the NF1-mutant Mewo and WM3918 human melanoma cells were inoculated subcutaneously in the right flank of nude mice. AMPKα2 knockout significantly increased the size of both Mewo and WM3918 xenografts (Figures 4A and 4B). These data together support that AMPKα2 negatively regulates melanoma anchorage-independent growth *in vitro* and tumor growth *in vivo*.

Decreased expression of AMPKα2 in melanoma brain metastasis

Melanoma has high rate of metastasis to the brain.¹⁹ Recently, melanoma brain metastases (MBMs) were found to have increased expression of the mitochondrial oxidative phosphorylation (OxPhos) metabolic pathway gene network, compared to extracranial metastases (ECMs).^{19,20} Given the close functional relationship between AMPK and OxPhos, we analyzed the expression of AMPKα1 (PRKAA1) and α2 (PRKAA2) genes in a cohort of patient-matched MBM and ECM tumor samples with NF1-mutant or NF1-WT status. RNA expression levels of PRKAA2 gene were much lower (~2.9-fold) in patient-matched MBMs versus ECMs tumor pairs of patients with NF1-mutant compared matched tumor pairs of patients with NF1-WT (1.1-fold; $p = 0.0452$; Figure 5A). In comparison, there were no significant difference in PRKAA1 gene expression ($p = 0.7059$) in tumor pairs of both patients with NF1-mutant and NF1-WT (Figure 5B). We also evaluated the expression of the two genes in tumor xenografts of the NF1-mutant Mewo cell line grown in mice as intracranial (ICr) and subcutaneous (SQ) tumors, established by direct injection as previously described.²⁰ Similar to the clinical samples, PRKAA2 expression levels were significantly lower (~1.5-fold; $p = 0.0126$) in ICr versus SQ tumors; PRKAA1 levels were small but significantly higher (0.4-fold; t test $p = 0.0009$) (Figure 5C). These results support that PRKAA2 expression in NF1-mutant melanomas is significantly decreased in intracranial tumors compared to extracranial tumors.

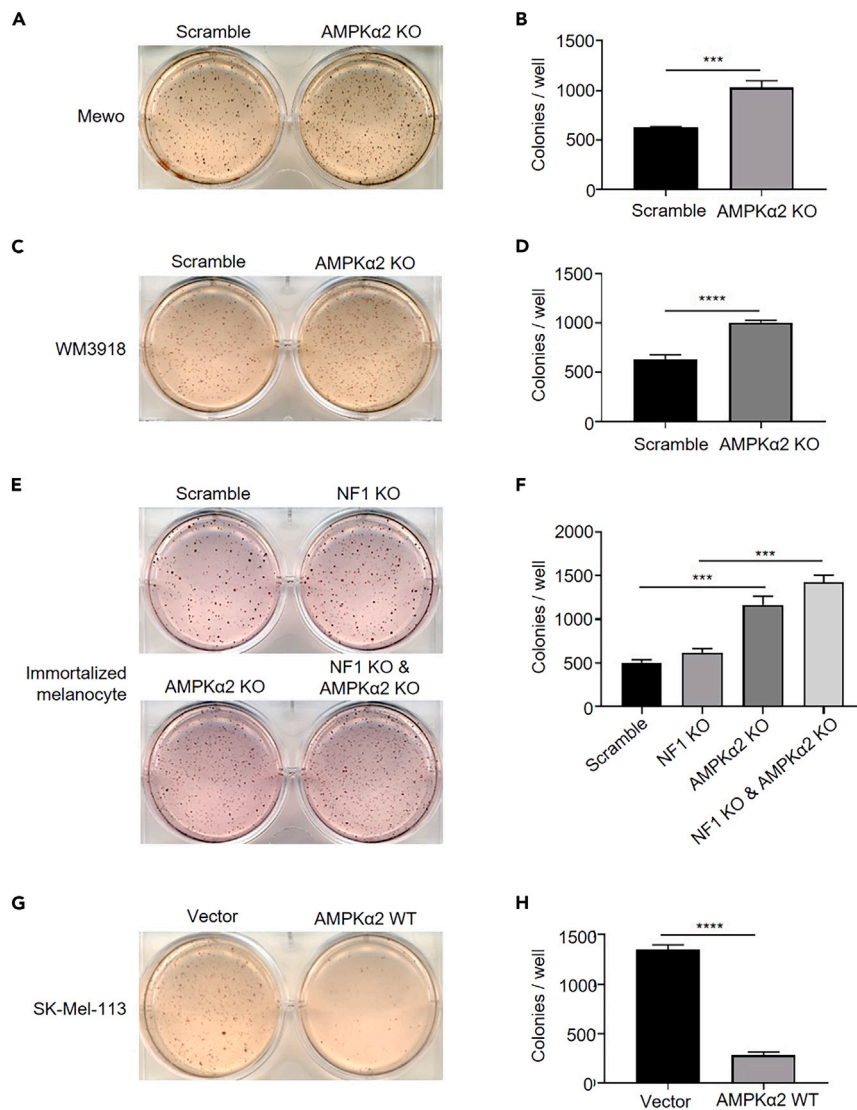


Figure 3. Effects of AMPK α 2 KO or overexpression on anchorage-independent growth of NF1-mutant melanoma cells and human immortalized melanocytes

(A–D) Scramble or AMPK α 2 KO Mewo (A, B) and WM3918 (C, D) melanoma cells were seeded triplicate in 6-well plates with soft agar and cultured for about 4 weeks.

(E and F) Scramble, NF1 KO, AMPK α 2 KO, or NF1 KO & AMPK α 2 KO immortalized melanocytes were seeded triplicate in 6-well plates with soft agar and cultured for about 4 weeks.

(G and H) SK-MEL-113 melanoma cells expressing AMPK α 2 or vector control were seeded triplicate in 6-well plates with soft agar and cultured for about 4 weeks. Three independent experiments were performed, and one of three experiments was shown. Colonies numbers were analyzed by ImageJ and data are presented as mean plus or minus standard deviation (SD). Statistical analyses using two-tailed Student t test performed on GraphPad Prism where, ***p < 0.001, ****p < 0.0001.

Loss of AMPK α 2 promotes brain metastasis of NF1-mutant melanoma cells in mice

To further characterize the effects of AMPK α 2 loss on MBM formation and growth *in vivo*, we performed intracardiac injection of luciferase-tagged Mewo cells with scrambled control or AMPK α 2 KO in NSG mice. We followed the growth and metastatic spread of the luciferase-labeled cells in the brain by imaging over a period of 36 days. Luminescence signals were observed in both periapical tissues and brain (Figure 6A). Interestingly, there was a significant increase of brain-specific luciferase signal (Figure 6B) and shorter survival (Figure 6C) in mice implanted with AMPK α 2 KO cells versus control cells, further supporting a role for AMPK α 2 loss in enhancing MBMs.

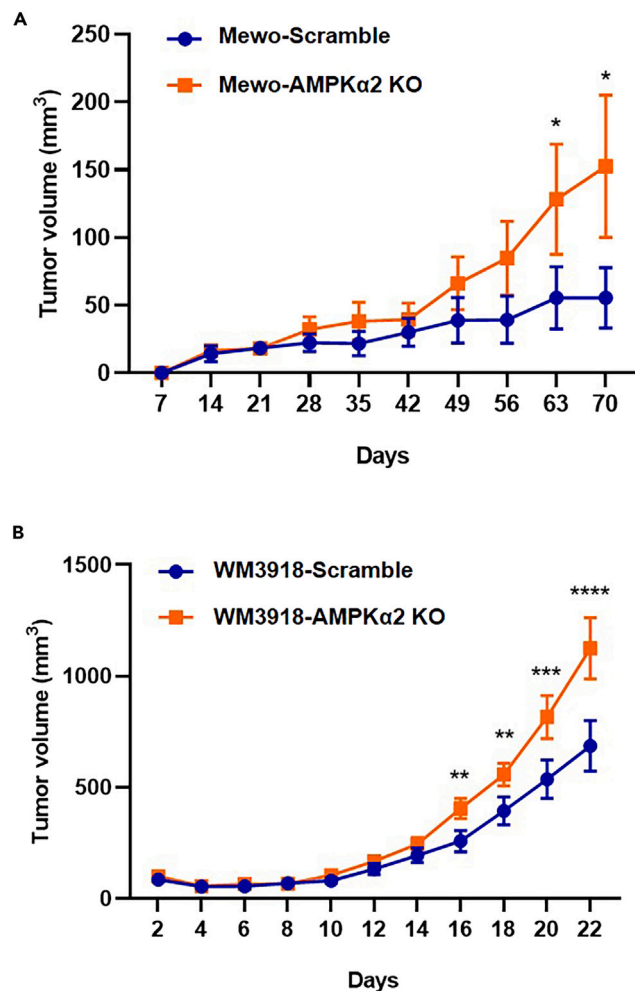


Figure 4. Loss of AMPK α 2 KO promotes xenograft growth of NF1-mutant melanoma cells in nude mice

(A) Scramble or AMPK α 2 KO Mewo cells were injected subcutaneously into the right lateral flank of nude mice (n = 6). (B) Scramble or AMPK α 2 KO WM3918 cells were injected subcutaneously into the right lateral flank of nude mice (n = 9). Tumor volumes were plotted as means plus or minus standard error of the mean (SEM). Statistical analyses using two-way ANOVA was performed on GraphPad Prism where, *p < 0.05, **p < 0.01, ***p < 0.001, ****p < 0.0001.

DISCUSSION

In this study, we report the frequent occurrence of PRKAA2 mutations, and their co-occurrence with NF1 mutations, in cutaneous melanomas. Furthermore, we have demonstrated that loss of AMPK α 2 promotes anchorage-independent growth of NF1-mutant melanoma cells *in vitro* and tumor growth *in vivo*. These findings support that AMPK α 2 is a tumor suppressor in NF1-mutant melanoma.

The roles of AMPK in carcinogenesis are complex.¹⁰ Activation of AMPK by the tumor suppressor LKB1 and the antitumor activities of AMPK activators support that AMPK may function as a tumor suppressor in cancer.^{21–24} However, some recent studies suggest that AMPK may also promote tumor growth in certain contexts. For example, AMPK has been shown to promote cancer cell survival under energy stress through regulating acetyl-CoA carboxylase (ACC)-dependent NADPH homeostasis and redox balance.²⁵ Inhibition of ACC1/2 by shRNA knockdown, which recapitulates AMPK activation and maintenance of NADPH levels, was shown to promote the growth of A549 and MCF7 xenografts in nude mice. In addition, knockdown of AMPK α 1 was shown to suppress breast tumor growth in xenograft models, probably via attenuation of SKP2 phosphorylation and subsequent Akt activation.¹¹ Findings from genetically engineered mouse model studies supporting either roles of AMPK exist,^{12–14} and in some cases, conflicting results have been reported in similar settings. For examples, double knockout

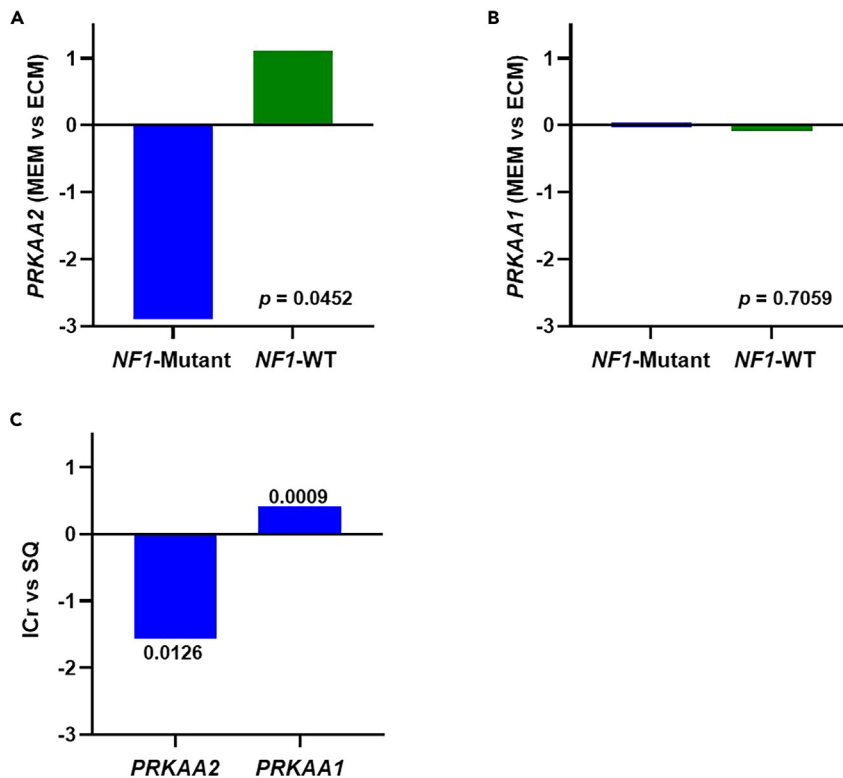


Figure 5. Downregulation of *PRKAA2* expression in melanoma brain metastasis

(A) Fold-changes in the expression of *PRKAA2* gene in MBM tumors versus ECM tumors from three pairs of patient-matched *NF1*-mutant melanoma samples (blue); and in twelve pairs of patient-matched *NF1*-WT melanoma samples (green).

(B) Fold-changes in the expression of *PRKAA1* gene in the same MBM versus ECM tumors from the same *NF1*-mutant (blue) and *NF1*-WT (green) melanoma samples as in (A).

(C) Fold changes in the expression of *PRKAA2* and *PRKAA1* genes in intracranial (ICr) versus subcutaneous (SQ) tumors of the *NF1*-mutant Mewo cell line grown in mice.

of *PRKAA1* and *PRKAA2* was reported to be detrimental to the growth of *Kras*^{G12D}*p53*^{-/-} non-small-cell lung cancer in one mouse model study,¹⁴ but was shown to promote tumor progression in *Kras*^{G12D} mouse model (with intact *p53*) in two other independent studies.^{26,27} It remains to be seen whether these tumor-promoting effects of AMPK are dependent on specific cellular contexts, tumor types, or AMPK complex $\alpha\beta\gamma$ subunit composition.

It is noteworthy that of the two catalytic AMPK subunits only $\alpha 2$ is frequently mutated and lost in melanoma (Figures 1A and 2A). Diana Vara-Ciruelos et al. previously also noted frequent mutations of AMPK $\alpha 2$ in skin cancer and melanoma datasets in the cBioPortal database.¹⁰ The two isoforms of the catalytic subunit of AMPK, AMPK $\alpha 1$ and AMPK $\alpha 2$, share many similarities in regulating metabolism and other cellular events. Both $\alpha 1$ and $\alpha 2$ proteins are expressed in melanocytes and melanomas at comparable levels. Although it has been suggested that $\alpha 1$ and $\alpha 2$ may differ in subcellular localization^{28–31} and regulation of their expression levels,^{32,33} overall very little is known about their biochemical and biological specificities, including substrate preferences. Loss of AMPK $\alpha 2$, but not $\alpha 1$, was previously reported to suppress H-RasV12 transformation of MEFs *in vitro* and tumorigenesis *in vivo*.³⁴ Ectopic expression of AMPK $\alpha 2$ was shown to suppress MCF-7 breast cancer cell proliferation and tumor growth.³⁵ Knockout of AMPK $\alpha 2$, but not $\alpha 1$, reduced levels of p27 via SKP2 in bladder cancer cells, which may contribute to the suppressive effects of AMPK $\alpha 2$ on bladder cancer tumor growth.³⁶ Our study here reveals that AMPK $\alpha 2$ serves as a tumor suppressor in melanoma. The LOF nature of cancer-associated *PRKAA2* mutations may explain why they frequently occur in *NF1*-mutant subtype of melanomas, instead of *BRAF*-mutant melanomas. We have previously shown that, in *BRAF*^{V600E} mutant melanomas, the activity of AMPK is inhibited by the

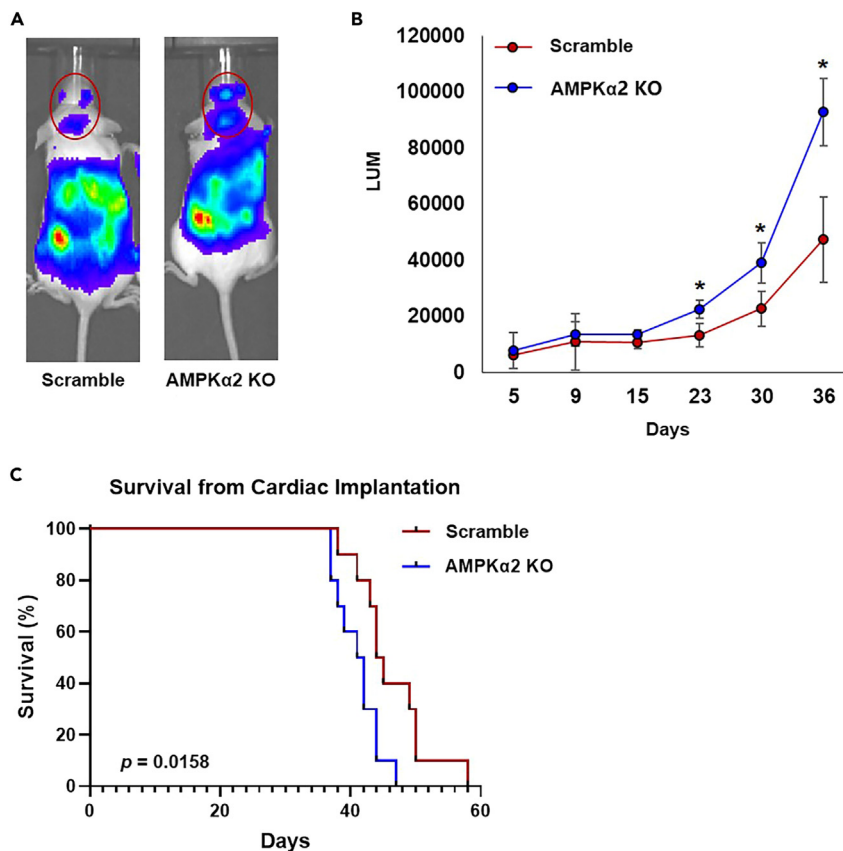


Figure 6. Loss of AMPK α 2 promotes brain metastasis of *NF1*-mutant melanoma in mice

(A) Luciferase-tagged Mewo cells with AMPK α 2 KO or scramble were implanted into NSG mice via intracardiac injections (n = 10). Luminescence signals were detected by imaging of mice after injecting them with luciferin at regular intervals as shown. The images shown are from 36 days following implantation.

(B) Brain-specific signal intensities were isolated in the anatomical location of the brain and plotted in a line graph. Significant differences between Mewo-Scramble and Mewo-AMPK α 2 KO groups are indicated by asterisks (*). Data points are average plus or minus standard deviation (SD). Statistical analyses using two-way ANOVA was performed on GraphPad Prism where, *p < 0.05.

(C) Kaplan-Meier survival analysis of the mice with cardiac implantation of Mewo-Scramble or Mewo-AMPK α 2 KO cells. Significance was determined by Mantel-Cox log rank test.

hyperactivation of BRAF-MEK-ERK signaling, via phosphorylation of LKB1 by ERK and p90Rsk.³⁷ Hence, it is conceivable that AMPK signaling is attenuated in *BRAF*-mutant melanomas through post-translational mechanisms and by a genetic mechanism in *NF1*-mutant melanomas.

Melanoma has one of the highest rates of brain metastasis of all solid tumor types.^{19,20,38} There remains an unmet need to develop more effective therapeutic strategies to treat MBMs.¹⁹ Our previous studies identified increased mitochondrial OxPhos in MBMs versus ECMs from the same patients, or in the same mice.²⁰ In this study, our analysis of patient samples and xenograft models revealed that MBMs also exhibit decreased levels of AMPK α 2 subunit expression. Furthermore, KO of AMPK α 2 promoted brain metastasis growth of *NF1*-mutant melanoma in NSG mice. Future studies utilizing immune-competent mouse models, such as syngeneic mouse melanoma models or genetically engineered mouse models, will help to further establish the role of AMPK α 2 loss MBMs. How AMPK α 2 regulates brain metastasis also remains to be determined. Given the central role of AMPK in metabolic regulation, it is conceivable that AMPK α 2 modulates the metabolic adaptation of metastatic melanoma cells in the brain microenvironment through its effectors. Future characterization of these metabolic pathways will likely reveal additional metabolic vulnerabilities of brain metastatic tumor cells and provide insights into developing new strategies for treatment of melanoma brain metastasis.

Limitation of the study

In this study, we observed that *PRKAA2* mutations occur at a high rate exclusively in melanoma and are associated with *NF1* mutations. Our analysis indicated both E168K and nonsense K379* mutations of *AMPK α 2* impaired its activity. Additional cancer-associated mutations of *AMPK α 2* should be characterized in the future. We also found that knockout of *AMPK α 2* promoted tumor growth and metastasis of *NF1*-mutated melanoma. While these results support a novel and important role, the molecular mechanisms underlying the regulation of growth and metastasis by *AMPK α 2* in *NF1*-mutated melanoma remain to be elucidated. There is also a need for additional studies to further characterize the role of *AMPK α 2* in MBMs, including in immune-competent models.

STAR★METHODS

Detailed methods are provided in the online version of this paper and include the following:

- KEY RESOURCES TABLE
- RESOURCE AVAILABILITY
 - Lead contact
 - Materials availability
 - Data and code availability
- EXPERIMENTAL MODEL AND STUDY PARTICIPANT DETAILS
 - *In vivo* animal studies
 - *In vitro* cellular studies
 - Cell lines used for genetic and transcription analysis
- METHOD DETAILS
 - Cell culture
 - CRISPR/Cas9-mediated gene knockout
 - Site-directed mutagenesis
 - Western blotting
 - Soft agar assays
 - Xenograft studies
 - DNA and RNA sequencing data analysis
- QUANTIFICATION AND STATISTICAL ANALYSIS

SUPPLEMENTAL INFORMATION

Supplemental information can be found online at <https://doi.org/10.1016/j.isci.2023.106791>.

ACKNOWLEDGMENTS

We thank Weiling Li, Chan Mu, and members of the Zheng Lab for assistance and helpful discussion on the manuscript. This work is supported by US National Institutes of Health (NIH, R01CA276448) (to B.Z. and Y.N.V.G.); a Sun Pharma-Society for Investigative Dermatology Mid-Career Investigator Award, the Melanoma Research Alliance, and funds from MGH (to B.Z.); and the Dr. Miriam and Sheldon G. Adelson Medical Research Foundation, the AIM at Melanoma Foundation, the MD Anderson SPORE in Melanoma (NIH/NCI P50CA221703), the American Cancer Society and the Melanoma Research Alliance, Cancer Fighters of Houston, the Anne and John Mendelsohn Chair for Cancer Research, and philanthropic contributions to the Melanoma Moon Shots Program of MD Anderson (to M.A.D.).

AUTHOR CONTRIBUTIONS

P.Y., M.A.D., Y.N.V.G., and B.Z. designed experiments; P.Y., M.L., E.D.G., D.T., S.T., C.-H.S., and Y.N.V.G. performed experiments; J.R. and Y.N.V.G. performed computational analysis; M.A.D., Y.N.V.G., and B.Z. provided supervision; all of the authors interpreted data and discussed results; and P.Y., Y.N.V.G., and B.Z. wrote the paper with input from all of the authors.

DECLARATION OF INTERESTS

M.A.D. has been a consultant to Roche/Genentech, Array, Pfizer, Novartis, BMS, GSK, Sanofi-Aventis, Vaccinex, Apexigen, Eisai, Iovance, Merck, and ABM Therapeutics, and he has been the PI of research grants to MD Anderson by Roche/Genentech, GSK, Sanofi-Aventis, Merck, Myriad, Oncothyreon, Pfizer, ABM Therapeutics, and LEAD Pharma. Y.N.V.G. has received funding from Calithera Biosciences.

Received: February 21, 2023

Revised: April 2, 2023

Accepted: April 26, 2023

Published: April 29, 2023

REFERENCES

- Shain, A.H., and Bastian, B.C. (2016). From melanocytes to melanomas. *Nat. Rev. Cancer* 16, 345–358. <https://doi.org/10.1038/nrc.2016.37>.
- Newell, F., Johansson, P.A., Wilmott, J.S., Nones, K., Lakis, V., Pritchard, A.L., Lo, S.N., Rawson, R.V., Kazakoff, S.H., Colebatch, A.J., et al. (2022). Comparative genomics provides etiologic and biological insight into melanoma subtypes. *Cancer Discov.* 12, 2856–2879. <https://doi.org/10.1158/2159-8290.CD-22-0603>.
- Maertens, O., Johnson, B., Hollstein, P., Frederick, D.T., Cooper, Z.A., Messiaen, L., Bronson, R.T., McMahon, M., Granter, S., Flaherty, K., et al. (2013). Elucidating distinct roles for NF1 in melanomagenesis. *Cancer Discov.* 3, 338–349. <https://doi.org/10.1158/2159-8290.CD-12-0313>.
- Shin, J., Padmanabhan, A., de Groh, E.D., Lee, J.-S., Haidar, S., Dahlberg, S., Guo, F., He, S., Wolman, M.A., Granato, M., et al. (2012). Zebrafish neurofibromatosis type 1 genes have redundant functions in tumorigenesis and embryonic development. *Dis. Model. Mech.* 5, 881–894. <https://doi.org/10.1242/dmm.009779>.
- Steinberg, G.R., and Hardie, D.G. (2023). New insights into activation and function of the AMPK. *Nat. Rev. Mol. Cell Biol.* 24, 255–272. <https://doi.org/10.1038/s41580-022-00547-x>.
- Shackelford, D.B., and Shaw, R.J. (2009). The LKB1-AMPK pathway: metabolism and growth control in tumour suppression. *Nat. Rev. Cancer* 9, 563–575. <https://doi.org/10.1038/nrc2676>.
- Casimiro, M.C., Di Sante, G., Di Rocco, A., Loro, E., Pupo, C., Pestell, T.G., Bisetto, S., Velasco-Velázquez, M.A., Jiao, X., Li, Z., et al. (2017). Cyclin D1 restrains oncogene-induced autophagy by regulating the AMPK-LKB1 signaling axis. *Cancer Res.* 77, 3391–3405. <https://doi.org/10.1158/0008-5472.CAN-16-0425>.
- Li, N., Wang, Y., Neri, S., Zhen, Y., Fong, L.W.R., Qiao, Y., Li, X., Chen, Z., Stephan, C., Deng, W., et al. (2019). Tankyrase disrupts metabolic homeostasis and promotes tumorigenesis by inhibiting LKB1-AMPK signalling. *Nat. Commun.* 10, 4363. <https://doi.org/10.1038/s41467-019-12377-1>.
- Wang, T., Guo, H., Li, Q., Wu, W., Yu, M., Zhang, L., Li, C., Song, J., Wang, Z., Zhang, J., et al. (2022). The AMPK-HOXB9-KRAS axis regulates lung adenocarcinoma growth in response to cellular energy alterations. *Cell Rep.* 40, 111210. <https://doi.org/10.1016/j.celrep.2022.111210>.
- Vara-Ciruelos, D., Russell, F.M., and Hardie, D.G. (2019). The strange case of AMPK and cancer: Dr jekyll or mr hyde? *Open Biol.* 9, 190099. <https://doi.org/10.1098/rsob.190099>.
- Han, F., Li, C.F., Cai, Z., Zhang, X., Jin, G., Zhang, W.N., Xu, C., Wang, C.Y., Morrow, J., Zhang, S., et al. (2018). The critical role of AMPK in driving Akt activation under stress, tumorigenesis and drug resistance. *Nat. Commun.* 9, 4728. <https://doi.org/10.1038/s41467-018-07188-9>.
- Chhipa, R.R., Fan, Q., Anderson, J., Muraleedharan, R., Huang, Y., Ciraolo, G., Chen, X., Waclaw, R., Chow, L.M., Khuchua, Z., et al. (2018). AMP kinase promotes glioblastoma bioenergetics and tumour growth. *Nat. Cell Biol.* 20, 823–835. <https://doi.org/10.1038/s41556-018-0126-z>.
- Cai, Z., Li, C.F., Han, F., Liu, C., Zhang, A., Hsu, C.C., Peng, D., Zhang, X., Jin, G., Rezaeian, A.H., et al. (2020). Phosphorylation of PDHA by AMPK drives TCA cycle to promote cancer metastasis. *Mol. Cell* 80, 263–278.e7. <https://doi.org/10.1016/j.molcel.2020.09.018>.
- Eichner, L.J., Brun, S.N., Herzog, S., Young, N.P., Curtis, S.D., Shackelford, D.B., Shokhirev, M.N., Leblanc, M., Vera, L.I., Hutchins, A., et al. (2019). Genetic analysis reveals AMPK is required to support tumor growth in murine Kras-dependent lung cancer models. *Cell Metabol.* 29, 285–302.e7. <https://doi.org/10.1016/j.cmet.2018.10.005>.
- Cerami, E., Gao, J., Dogrusoz, U., Gross, B.E., Sumer, S.O., Aksoy, B.A., Jacobsen, A., Byrne, C.J., Heuer, M.L., Larsson, E., et al. (2012). The cBio Cancer Genomics Portal: an open platform for exploring multidimensional cancer genomics data. *Cancer Discov.* 2, 401–404. <https://doi.org/10.1158/2159-8290.CD-12-0095>.
- Gao, J., Aksoy, B.A., Dogrusoz, U., Dresdner, G., Gross, B., Sumer, S.O., Sun, Y., Jacobsen, A., Sinha, R., Larsson, E., et al. (2013). Integrative analysis of complex cancer genomics and clinical profiles using the cBioPortal. *Sci. Signal.* 6, p11. <https://doi.org/10.1126/scisignal.2004088>.
- Cascone, T., McKenzie, J.A., Mbofung, R.M., Punt, S., Wang, Z., Xu, C., Williams, L.J., Wang, Z., Bristow, C.A., Carugo, A., et al. (2018). Increased tumor glycolysis characterizes immune resistance to adoptive T cell therapy. *Cell Metabol.* 27, 977–987.e4. <https://doi.org/10.1016/j.cmet.2018.02.024>.
- Andrews, M.C., Oba, J., Wu, C.J., Zhu, H., Karpinet, T., Creasy, C.A., Forget, M.A., Yu, X., Song, X., Mao, X., et al. (2022). Multimodal molecular programs regulate melanoma cell state. *Nat. Commun.* 13, 4000. <https://doi.org/10.1038/s41467-022-31510-1>.
- Karz, A., Dimitrova, M., Kleffman, K., Alvarez-Breckenridge, C., Atkins, M.B., Boire, A., Bosenberg, M., Brastianos, P., Cahill, D.P., Chen, Q., et al. (2022). Melanoma central nervous system metastases: an update to approaches, challenges, and opportunities. *Pigment Cell Melanoma Res.* 35, 554–572. <https://doi.org/10.1111/pcmr.13059>.
- Fischer, G.M., Jalali, A., Kircher, D.A., Lee, W.-C., McQuade, J.L., Haydu, L.E., Joon, A.Y., Reuben, A., de Macedo, M.P., Carapeto, f.c.l., et al. (2019). Molecular profiling reveals unique immune and metabolic features of melanoma brain metastases. *Cancer Discov.* 9, 628–645. <https://doi.org/10.1158/2159-8290.CD-18-1489>.
- Trousil, S., Chen, S., Mu, C., Shaw, F.M., Yao, Z., Ran, Y., Shakuntala, T., Merghoub, T., Manstein, D., Rosen, N., et al. (2017). Phenformin enhances the efficacy of ERK inhibition in NF1-mutant melanoma. *J. Invest. Dermatol.* 137, 1135–1143. <https://doi.org/10.1016/j.jid.2017.01.013>.
- Yuan, P., Ito, K., Perez-Lorenzo, R., Del Guzzo, C., Lee, J.H., Shen, C.-H., Bosenberg, M.W., McMahon, M., Cantley, L.C., and Zheng, B. (2013). Phenformin enhances the therapeutic benefit of BRAF(V600E) inhibition in melanoma. *Proc. Natl. Acad. Sci. USA* 110, 18226–18231. <https://doi.org/10.1073/pnas.1317577110>.
- Grenier, A., Poulain, L., Mondesir, J., Jacquell, A., Bosc, C., Stuani, L., Mouche, S., Larrue, C., Sahal, A., Birsén, R., et al. (2022). AMPK-PERK axis represses oxidative metabolism and enhances apoptotic priming of mitochondria in acute myeloid leukemia. *Cell Rep.* 38, 110197. <https://doi.org/10.1016/j.celrep.2021.110197>.
- Faubert, B., Boily, G., Izreig, S., Griss, T., Samborska, B., Dong, Z., Dupuy, F., Chambers, C., Fuerth, B.J., Viollet, B., et al. (2013). AMPK is a negative regulator of the Warburg effect and suppresses tumor growth in vivo. *Cell Metabol.* 17, 113–124. <https://doi.org/10.1016/j.cmet.2012.12.001>.
- Jeon, S.-M., Chandel, N.S., and Hay, N. (2012). AMPK regulates NADPH homeostasis to promote tumour cell survival during energy stress. *Nature* 485, 661–665. <https://doi.org/10.1038/nature11066>.
- Gao, Y., Päivinen, P., Tripathi, S., Domènech-Moreno, E., Wong, I.P.L., Vaahtomeri, K., Nagaraj, A.S., Talwelkar, S.S., Foretz, M., Verschuren, E.W., et al. (2022). Inactivation of AMPK leads to attenuation of antigen presentation and immune evasion in lung adenocarcinoma. *Clin. Cancer Res.* 28, 227–237. <https://doi.org/10.1158/1078-0432.ccr-21-2049>.

27. La Montagna, M., Shi, L., Magee, P., Sahoo, S., Fassan, M., and Garofalo, M. (2021). AMPK α loss promotes KRAS-mediated lung tumorigenesis. *Cell Death Differ.* 28, 2673–2689. <https://doi.org/10.1038/s41418-021-00777-0>.
28. Schmitt, D.L., Curtis, S.D., Lyons, A.C., Zhang, J.-F., Chen, M., He, C.Y., Mehta, S., Shaw, R.J., and Zhang, J. (2022). Spatial regulation of AMPK signaling revealed by a sensitive kinase activity reporter. *Nat. Commun.* 13, 3856. <https://doi.org/10.1038/s41467-022-31190-x>.
29. Chauhan, A.S., Zhuang, L., and Gan, B. (2020). Spatial control of AMPK signaling at subcellular compartments. *Crit. Rev. Biochem. Mol. Biol.* 55, 17–32. <https://doi.org/10.1080/10409238.2020.1727840>.
30. Quentin, T., Kitz, J., Steinmetz, M., Poppe, A., Bär, K., and Krätzner, R. (2011). Different expression of the catalytic alpha subunits of the AMP activated protein kinase—an immunohistochemical study in human tissue. *Histol. Histopathol.* 26, 589–596. <https://doi.org/10.14670/hh-26.589>.
31. Cheratta, A.R., Thayyullathil, F., Hawley, S.A., Ross, F.A., Atrih, A., Lamont, D.J., Pallichankandy, S., Subburayan, K., Alakkal, A., Rezgui, R., et al. (2022). Caspase cleavage and nuclear retention of the energy sensor AMPK- α 1 during apoptosis. *Cell Rep.* 39, 110761. <https://doi.org/10.1016/j.celrep.2022.110761>.
32. Prastowo, S., Amin, A., and Soheli, M.H. (2017). Identifying candidate microRNAs in microRNA-AMPK gene interaction regulating lipid accumulation of bovine granulosa cell luteinization: an in silico study. In *Proceeding of the 1st international conference on tropical agriculture*, A. Isnansetyo and T. Nuringtyas, eds. (Springer), pp. 431–438. https://doi.org/10.1007/978-3-319-60363-6_45.
33. Suzuki, A., Okamoto, S., Lee, S., Saito, K., Shiuchi, T., and Minokoshi, Y. (2007). Leptin stimulates fatty acid oxidation and peroxisome proliferator-activated receptor alpha gene expression in mouse C2C12 myoblasts by changing the subcellular localization of the alpha2 form of AMP-activated protein kinase. *Mol. Cell Biol.* 27, 4317–4327. <https://doi.org/10.1128/mcb.02222-06>.
34. Phoenix, K.N., Devarakonda, C.V., Fox, M.M., Stevens, L.E., and Claffey, K.P. (2012). AMPK α 2 suppresses murine embryonic fibroblast transformation and tumorigenesis. *Genes Cancer* 3, 51–62. <https://doi.org/10.1177/1947601912452883>.
35. Fox, M.M., Phoenix, K.N., Kopsiaftis, S.G., and Claffey, K.P. (2013). AMP-Activated Protein Kinase α 2 isoform suppression in primary breast cancer alters AMPK growth control and apoptotic signaling. *Genes Cancer* 4, 3–14. <https://doi.org/10.1177/1947601913486346>.
36. Kopsiaftis, S., Sullivan, K.L., Garg, I., Taylor, J.A., III, and Claffey, K.P. (2016). AMPK α 2 regulates bladder cancer growth through SKP2-mediated degradation of p27. *Mol. Cancer Res.* 14, 1182–1194. <https://doi.org/10.1158/1541-7786.mcr-16-0111>.
37. Zheng, B., Jeong, J.H., Asara, J.M., Yuan, Y.-Y., Granter, S.R., Chin, L., and Cantley, L.C. (2009). Oncogenic B-RAF negatively regulates the tumor suppressor LKB1 to promote melanoma cell proliferation. *Mol. Cell* 33, 237–247. <https://doi.org/10.1016/j.molcel.2008.12.026>.
38. Caulfield, J.I., and Kluger, H.M. (2022). Emerging studies of melanoma brain metastasis. *Curr. Oncol. Rep.* 24, 585–594. <https://doi.org/10.1007/s11912-022-01237-9>.
39. Davies, M.A., Stemke-Hale, K., Lin, E., Tellez, C., Deng, W., Gopal, Y.N., Woodman, S.E., Calderone, T.C., Ju, Z., Lazar, A.J., et al. (2009). Integrated molecular and clinical analysis of AKT activation in metastatic melanoma. *Clin. Cancer Res.* 15, 7538–7546. <https://doi.org/10.1158/1078-0432.ccr-09-1985>.
40. Sloane, R.A.S., White, M.G., Witt, R.G., Banerjee, A., Davies, M.A., Han, G., Burton, E., Ajami, N., Simon, J.M., Bernatchez, C., et al. (2021). Identification of MicroRNA-mRNA networks in melanoma and their association with PD-1 checkpoint blockade outcomes. *Cancers* 13, 5301. <https://doi.org/10.3390/cancers13215301>.
41. Shalem, O., Sanjana, N.E., Hartenian, E., Shi, X., Scott, D.A., Mikkelsen, T., Heckl, D., Ebert, B.L., Root, D.E., Doench, J.G., and Zhang, F. (2014). Genome-scale CRISPR-Cas9 knockout screening in human cells. *Science* 343, 84–87. <https://doi.org/10.1126/science.1247005>.
42. Zheng, B., and Cantley, L.C. (2007). Regulation of epithelial tight junction assembly and disassembly by AMP-activated protein kinase. *Proc. Natl. Acad. Sci. USA* 104, 819–822. <https://doi.org/10.1073/pnas.0610157104>.

STAR★METHODS

KEY RESOURCES TABLE

REAGENT or RESOURCE	SOURCE	IDENTIFIER
Antibodies		
NF1 Polyclonal Antibody	Bethyl Laboratories	Cat#A300-140A
Anti-AMPK α 1 Antibody	Upstate®	Cat#07-350
Anti-AMPK α 2 Antibody	Upstate®	Cat#07-363
Phospho-Acetyl-CoA Carboxylase (Ser79) Antibody	Cell Signaling Technology	Cat#3661; RRID:AB_330337
Acetyl-CoA Carboxylase (C83B10) Rabbit mAb	Cell Signaling Technology	Cat#3676; RRID:AB_2219397
β -Tubulin (9F3) Rabbit mAb	Cell Signaling Technology	Cat#2128; RRID:AB_823664
Bacterial and virus strains		
Subcloning Efficiency DH5 α ™	Invitrogen	18265017
One Shot™ Stb13™	Invitrogen	C737303
Chemicals, peptides, and recombinant proteins		
AICAR (5-Aminoimidazole-4-carboxamide-1- β -D-ribofuranosyl 3':5'-cyclic-monophosphate)	Toronto Research Chemicals	Cat#A440500; CAS: 35908-14-6
puromycin	Sigma-Aldrich	P8833, CAS: 58-58-2
hygromycin	Roche	10842555001; CAS: 31282-04-9
iodonitrotetrazolium chloride	Sigma	I8377; CAS: 146-69-9
IBMX	Sigma	I7018; CAS:28822-58-4
TPA	Sigma	P8139; CAS: 16561-29-8
dbcAMP	Sigma	D0627; CAS: 16980-89-5
Na ₃ VO ₄	Sigma	Cat#450243; CAS:13721-39-6
Critical commercial assays		
QuickChange Lightning Site-Directed Mutagenesis Kit	Aligent	Cat#210519
Plasmid Maxi Kit (25)	Qiagen	Cat#12163
Plasmid Mini Kit (100)	Qiagen	Cat#12125
Bradford Assay kit	Pierce	23246
ECL detection reagent	Pierce	PI32106
Deposited data		
Whole exome DNA sequencing of melanoma moonshot cell lines	Fischer, et al. ¹⁹	N/A
RNA sequencing of melanoma moonshot cell lines	Sloane, et al. ⁴¹	N/A
Experimental models: Cell lines		
Mewo	Gifted from Lynda Chin	N/A
WM3918	From MSKCC	N/A
SK-Mel-113	From MSKCC	N/A
SK-Mel-217	From MSKCC	N/A
SK-Mel-103	From MSKCC	N/A
WM88	Gifted from Lynda Chin	N/A
M308	Gifted from Antoni Ribas	N/A

(Continued on next page)

Continued

REAGENT or RESOURCE	SOURCE	IDENTIFIER
Immortalized human melanocyte	Gifted from Dr. Hans R. Widlund	N/A
Immortalized AMPK α 1/ α 2-null MEF	Gifted from Dr. Benoit Violette	N/A
Experimental models: Organisms/strains		
NCR nude mice	Charles River Laboratories, Wilmington, MA	N/A
NSG mice	Charles River Laboratories, Wilmington, MA	N/A
Oligonucleotides		
gRNA PRKAA2: GAAGATCGGACACTACGTGC	Integrated DNA technology	N/A
gRNA PRKAA1: GAAGATCGGCCACTACATTC	Integrated DNA technology	N/A
gRNA NF1: AGTCAGTACTGAGCACAACA	Integrated DNA technology	N/A
gRNA human rosa26: AGGCCGCACCCTTCTCCGG	Integrated DNA technology	N/A
Recombinant DNA		
LentiCRISPRv2	Addgene	Plasmid#52961
LentiCRISPRv2 hygro	Addgene	Plasmid#98291
psPAX2	Addgene	Plasmid#12260
pCMV-VSV-G	Addgene	Plasmid#8454
pLHCX	Clontech	N/A
pLHCX-AMPK α 2-WT	This paper	N/A
Ampho Retrovirus Packaging Vector	Clontech	N/A
Software and algorithms		
GraphPad Prism 8	GraphPad	N/A
ImageJ	NIH	https://ImageJ.nih.gov/ij/
Living Image software	Perkin Elmer	N/A
Other		
RPMI 1640	Gibco™	Cat#21870092
DMEM high glucose	Gibco™	Cat#10313039
Fetal Bovine Serum - Premium	R&D systems	S11150
0.05%Trypsin-EDTA	Gibco™	Cat#25300120
Ham's F-12	Sigma	N6658
Pen-Strep	Gibco™	Cat#15140122
L-glutamine	Gibco™	Cat#25030081

RESOURCE AVAILABILITY**Lead contact**

Further information and requests for resources and reagents should be directed to and will be fulfilled by the lead contact, Dr. Bin Zheng (bin.zheng@cbrc2.mgh.harvard.edu).

Materials availability

This study did not generate any new materials.

Data and code availability

- All data reported in this paper will be shared by the [lead contact](#) upon request.
- This paper does not report original code.

- Any additional information required to reanalyze the data reported in this paper is available from the [lead contact](#) upon request.

EXPERIMENTAL MODEL AND STUDY PARTICIPANT DETAILS

In vivo animal studies

Six to eight weeks-aged female mice were used for animal studies. NCR nude mice, purchased from Charles River Laboratories (Wilmington, MA), were used for subcutaneous xenografts studies. NSG mice were used for brain metastasis study. All animal experiments were performed by following MGH and MDACC Animal Care and Use Committee guidelines.

In vitro cellular studies

Human melanoma cell lines (Mewo, WM88, M308, WM3918, SK-Mel-113, SK-Mel-103 and SK-Mel-217), HEK293T, immortalized human melanocytes, and Immortalized mouse embryonic fibroblast (MEF) with AMPK α 1/ α 2-null were used in this study. Cells were cultured at 37°C in humidified atmosphere containing 5% CO₂.

Cell lines used for genetic and transcription analysis

Patient-derived melanoma cell lines were established as part of the MDACC Melanoma Moonshot Program and TIL (tumor infiltrating lymphocyte) Therapy Program under an institutional review board-approved laboratory protocol with informed consent (LAB06-0755), and have been reported previously.^{17,18} Authentication of these cell lines was performed by short tandem repeat (STR) profiling as previously described.³⁹ Whole exome DNA sequencing analysis of melanoma moonshot cell lines was performed previously²⁰ and cell lines with inactivating mutations in *NF1* and *PRKAA2* genes were identified. RNA sequencing of the melanoma moonshot cell lines was reported previously,⁴⁰ and normalized mRNA [FPKM] counts were assessed.

METHOD DETAILS

Cell culture

Human melanoma cell lines, Mewo, WM88, M308, WM3918, SK-Mel-113, SK-Mel-103 and SK-Mel-217 were obtained²¹ and maintained in our lab. All above cells were cultured in RPMI 1640 containing 10% FBS and 1% penicillin/streptomycin/glutamine. Immortalized human melanocyte (Pmel/hTERT/CDK4/p53DD cell line) was cultured in Ham's F12 containing 7% FBS, 1% penicillin/streptomycin, 50 ng/mL TPA, 1×10^{-4} M IBMX, 1.0 μ M Na₂VO₄ and 1×10^{-4} M dbcAMP. Immortalized AMPK α 1/ α 2-null MEFs and HEK293T cells were cultured in high glucose DMEM containing 10% FBS and 1% penicillin/streptomycin/glutamine.

CRISPR/Cas9-mediated gene knockout

Guide RNAs (gRNAs) targeting *PRKAA2*, *PRKAA1* were designed on the website: <http://crispor.tefor.net>. gRNA targeting *NF1* was cited from Ophir Shalem et al.⁴¹ gRNA targeting human *rosa26* was used as a control. Sense and antisense oligonucleotides were annealed and then cloned into lentiCRISPR v2 according to the "Target Guide Sequence Cloning Protocol" Provided by the laboratory of Dr. Feng Zhang. Transfection and lentiviral infection were performed as previously described.²¹ Briefly, for lentiviral infection, HEK293T cells were co-transfected with lentiCRISPR v2 constructs, psPAX2 and pCMV-VSV-G. The lentiviral particles were collected and filtered at 48h and 72h, respectively. Target cells were infected with lentiviral particles with 10 μ g/mL polybrene. Stable populations were selected and maintained with 50 μ g/mL hygromycin, or 1 μ g/mL puromycin.

Site-directed mutagenesis

Site-directed mutagenesis was performed and guided with QuickChange Lightning Site-Directed Mutagenesis Kit. Constructs of AMPK WT or mutants and vector were prepared by Maxiprep (Qiagen). For retroviral transfection, amphotropic retrovirus were generated as described previously.⁴² Briefly, HEK293T cells were co-transfected with AmpHo and pLHCX or pLHCX-AMPK α 2-WT, pLHCX-AMPK α 2 Mutants (E168K or K379*), respectively. The viral particles were collected and filtered at 48 h and 72 h, respectively. Target cells were infected with viral particles with 10 μ g/mL polybrene twice. Stable populations were obtained

and maintained by selection with 100 $\mu\text{g}/\text{mL}$ hygromycin (for MEF) or 200 $\mu\text{g}/\text{mL}$ hygromycin (for SK-MeL-113).

Western blotting

Western blotting was performed as previously described.³⁷ Briefly, the cells were washed twice with ice-cold PBS quickly, and thrown into liquid nitrogen tank for about 1 min. Then the cells were lysed in a modified lysis buffer (50 mM Tris pH 7.4, 150 mM NaCl, 1% NP-40, 1 mM EDTA, 50 mM NaF, 10 mM β -glycero-phosphate, 10 nM calyculin A, 1 mM Na_3VO_4 , and protease inhibitors) with gentle rotation in cold room for 30 min. After centrifugation at 12000 rpm for 15 min, the supernatant was isolated and protein concentration was detected by Bradford method. For western blotting, protein samples were separated on 6%–10% SDS-PAGE and transferred to PVDF membrane. Membranes were blocked in TBST containing 3% BSA or 5% nonfat milk. The primary antibodies against NF1, AMPK α 1, AMPK α 2, p-ACC, ACC, Tubulin were used. All primary antibodies were used at a 1:1,000 dilution by TBST.

Soft agar assays

The soft agar assays were performed as previously described.³⁷ Briefly, the bottom agarose (0.6%) was plated in 6-well culture plates beforehand. Cells were suspended in 0.3% agarose in complete medium and plated in 6-well plates covered with solidified 0.6% agarose. Mewo-Scramble or AMPK α 2 KO, WM3918-Scramble or AMPK α 2 KO, immortalized human melanocyte-Scramble, NF1 KO, AMPK α 1/ α 2 KO or NF1KO & AMPK α 1/ α 2 KO, SK-MeL-113 vector or AMPK α 2 WT (about 7500 cells/well) were seeded in 6-well plates, triplicates were plated for each experiment. Once the agarose was solidified, it was soaked in the corresponding culture medium and feed twice per week, until the colonies were visible (about 30–40 days, respectively). The colonies were stained with 0.01% iodinitrotetrazolium chloride in PBS for 24 h and photographed. The ImageJ software was used to analysis the numbers of colonies. Three independent experiments were proceeded for each cell line.

Xenograft studies

All animal experiments were performed by following MGH and MDACC Animal Care and Use Committee guidelines. For xenograft models, 6 weeks female NCR nude mice were purchased from Charles River Laboratories (Wilmington, MA). Animals were allowed a 1-week adaptation period after arrival. Mewo-Scramble or Mewo-AMPK α 2 KO cells (2×10^6), WM3918-Scramble or WM3918-AMPK α 2 KO cells (1×10^5) cells, in 0.2 mL of basal culture medium, were injected subcutaneously into the right lateral flanks. There are 6 mice per group for Mewo, 9 mice per group for WM3918. Tumor volumes were calculated from caliper measurements by using the following ellipsoid formula: $(D \times d^2)/2$, in which D represents the large diameter of the tumor, and d represents the small diameter. For brain metastasis experiments, generation of intra-cranial (ICr) and subcutaneous (SQ) tumors of Mewo cell line in mice were described previously.²⁰ Mewo-Scramble cells or Mewo-AMPK α 2 KO cells (1×10^5) stably expressing luciferase were injected into the left ventricle of the heart of NSG mice ($n = 10/\text{group}$). Tumor burden in the mice was detected by bioluminescence using an IVIS imaging system continuously on the indicated days over a period of 36 days following implantation. Each time, the mice were anesthetized with isoflurane and whole-body luminescence signals were detected in 10 min after injecting with D-luciferin. All mice were euthanized after conclusion of the experiment, and Living Image software (Perkin Elmer) was used to isolate luminescence signal intensities in different anatomical locations of the animals. Brain location-specific signal intensities were quantified and plotted in a line graph. Significant differences between the two groups are indicated by asterisks (*). Data points are average \pm standard deviation. Kaplan Meier survival analysis was performed using the Mantel-Cox Log rank testing in Graphpad Prism.

DNA and RNA sequencing data analysis

Whole exome DNA sequencing and RNA sequencing data from MBM and ECM patient tumor samples, and RNA sequencing data from Mewo ICr and SQ xenograft tumors grown in mice have been reported earlier.^{20,40} Fold changes of the normalized counts of *PRKAA1* and *PRKAA2* gene transcripts from *NF1*-mutant patient tumors and the mice xenografted with Mewo tumors were assessed. Whole exome DNA sequencing analysis of melanoma moonshot cell lines was performed previously²⁰ and cell lines with inactivating mutations in *NF1* and *PRKAA2* genes were identified. RNA sequencing of the melanoma moonshot cell lines was reported previously,⁴² and normalized mRNA [FPKM] counts were assessed.

QUANTIFICATION AND STATISTICAL ANALYSIS

All data represent mean \pm SD/SEM. Statistical evaluations of anchorage-independent growth were conducted using two-tailed Student *t* test. Statistical analyses of xenograft and IVIS were conducted using two-way ANOVA. *p* values less than 0.05 were considered statistically significant. All data were performed using GraphPad Prism 8.0 software unless otherwise noted.